

Spectroscopic and Density Functional Theory Studies of a New Rosane Type Diterpenoid from *Stachys parviflora*

Umar Farooq^{1,*}, Khurshid Ayub^{1,2}, Muhammad Ali Hashmi¹,
Rizwana Sarwar¹, Afsar Khan^{1,**}, Saleha Suleman Khan³,
Ajmal Khan¹ and Mumtaz Ali⁴

¹ Department of Chemistry, COMSATS Institute of Information Technology, Abbottabad-22060, Pakistan

² Department of Chemistry, College of Science, King Faisal University, Al-Hafouf, 31982, Saudi Arabia

³ H. E. J. Research Institute of Chemistry, International Center for Chemical and Biological Sciences,
University of Karachi, Karachi-75270, Pakistan

⁴ Department of Chemistry, University of Malakand, Chakdara, Dir (L), Pakistan

(Received May 15, 2014; Revised September 18, 2014; Accepted September 23, 2014)

Abstract: A rosane type diterpenoid has been isolated from the ethyl acetate soluble fraction of *Stachys parviflora*. The structure elucidation was based primarily on 1D- and 2D-NMR techniques including correlation spectroscopy (COSY), heteronuclear multiple quantum coherence (HMQC), heteronuclear multiple bond correlation (HMBC), and nuclear Overhauser effect spectroscopy (NOESY). Density functional theory calculations have been performed to gain insight into the geometric, electronic and spectroscopic properties of the isolated diterpenoid. The geometries, vibrational spectrum and electronic properties were modeled at B3LYP/6-31G(d) and the theoretical data correlated nicely with the experimental values. Simulated chemical shifts at B3LYP/6-311+G(2d,p) showed much better correlation with the experimental chemical shifts, compared to B3LYP/6-31G(d) and WP04/6-31G(d).

Keywords: *Stachys parviflora*; diterpenoid; B3LYP; GIAO; DFT. © 2015 ACG Publications. All rights reserved.

1. Introduction

Stachys parviflora belongs to the Lamiaceae (Mint) family, distributed in the tropical and temperate regions of Pakistan.[1] The species of the genus *Stachys* are used for the treatment of diarrhea, fever, sore mouth and throat, internal bleeding, and weakness of the liver and heart. These are reported to possess anti-mutagenic, anti-allergic [2] and anticancer [3] activities as well. Previous phytochemical investigations on different species of the genus revealed the presence of alkaloids, glucosides, terpenoids, flavonoids, phenethyl alcohol glycosides and saponins [1] while *Stachys parviflora* was still unexplored phytochemically. Considering the medicinal importance attributed to the species of the genus *Stachys* and no phytochemical work on the species *Stachys parviflora*, it was decided to investigate its chemical

* Corresponding author: E-Mail: umarf@ciit.net.pk; afsarhej@gmail.com; Phone:+92-992-383591-5

constituents. In this paper we describe the isolation and characterization of a new rosane type diterpenoid from *Stachys parviflora*.

2. Materials and Methods

2.1. Experimental

2.1.1. Plant Material

The air-dried whole plant of *Stachys parviflora* was collected from Abbottabad, Pakistan, in March 2012. The plant was identified by Dr. Manzoor Ahmad (Taxonomist), Department of Botany, Post-Graduate College, Abbottabad. A voucher specimen (No. 14230) has been submitted in the herbarium of the same department.

2.1.2. Extraction and Isolation

The whole plant (14 kg) was grinded and extracted with methanol at room temperature. The extract was evaporated under reduced pressure to obtain a crude extract. The resulting methanolic extract (720 g) was suspended in water and successively partitioned between different solvents to get *n*-hexane (85 g), chloroform (70 g), ethyl acetate (50 g), *n*-butanol (95 g), and aqueous fractions (150 g).

The ethyl acetate fraction was further subjected to column chromatography over a silica gel column using *n*-hexane with a gradient of ethyl acetate up to 100% followed by methanol. Eight sub-fractions were collected through column chromatography. Sub-fraction 5 was further subjected to flash chromatography and eluted with EtOAc/*n*-hexane 25:75 which afforded compound 1 (9.3 mg).

2.1.3. General Experimental Procedure

Column chromatography was performed using silica gel (70-230 mesh); (E-Merck) and silica gel (230-400 mesh); (E-Merck). Analytical TLC was performed on precoated plates (silica gel 60 F₂₅₄). Optical rotations were recorded using a Jasco DIP-360 digital polarimeter. UV and IR spectra were recorded with UV-240 and JASCO-320-A spectrophotometers, respectively. EI-MS and HR-EI-MS were recorded on a double-focusing Varian MAT-312 spectrometer. The ¹H- and ¹³C-NMR spectra were recorded on a Bruker AMX-400 spectrometer, while 2D-NMR spectra were recorded on Bruker AMX-500 MHz spectrometer. Chemical shifts in parts per million (δ) relative to TMS as an internal standard, and scalar couplings (*J*) were reported in Hz.

2.2 Computational Details

All calculations were performed with Gaussian 09 suite of programs [4]. Geometries were optimized without any symmetry constraints at hybrid B3LYP method using 6-31G(d) [5] basis set. The B3LYP method is employed here which consists of three parameter hybrid functional of Becke [6] in conjunction with the correlation functional of Lee, Yang, and Parr [7]. The B3LYP method provides a nice balance between cost and accuracy, and is known to perform very well for the prediction of geometries of a number of synthetic and natural products.[8] An initial guess of the geometry of the diterpenoid is based on the stereochemistry assigned through 1D and 2D NMR characterization. The diterpenoid does not have any conformational flexibility except around the dihedral angle C14-C13-C15-C16. The dihedral angle C14-C13-C15-C16 has been scanned at 10 degrees step, to find the lowest energy conformer. Two minima were located on the potential energy surface; a local minimum (**1b**) at the dihedral angle of -126.2° and the global minimum (**1a**) at the dihedral angle of +120.0°. The energy difference between the local minimum and global minimum is 0.16 kcal mol⁻¹. Since the spectroscopic and electronic properties of these two minima are very similar therefore, discussion is only limited to the global minimum (**1a**), hereby referred as **1**. Each optimized structure was confirmed by frequency analysis at the same level (B3LYP/6-31G(d)) as a true minimum (no imaginary frequency). The simulated vibrational spectrum was scaled with a commonly accepted scaling

factor of 0.9613 (for B3LYP/6-31G(d)) [9]. TD-DFT calculations have been performed at TD-B3LYP/6-31G(d) level (solvent = Methanol) for the simulation of UV-Vis spectrum. Both singlet and triplet excitations were also taken into account for the simulation of UV-Vis spectrum. Three methods were evaluated for the simulation of ^1H NMR spectrum; B3LYP/6-31G(d), B3LYP/6-311+G(2d,p) and Cramer reparameterized WP04/6-31G(d). The simulated chemical shifts were then scaled with the appropriate scaling factors [10-12] and are given in the supporting information (Table SI 2). The chemical shifts simulated at B3LYP/6-311+G(2d,p) correlated much better with the experimental chemical shift values, compared to the other two levels. The reported ^1H - and ^{13}C -NMR theoretical chemical shifts in this manuscript have been calculated at B3LYP through Gauge Independent Atomic Orbital (GIAO) method at 6-311+G(2d,p) basis set on the B3LYP/6-31G(d) optimized geometries. The UV-Vis and NMR spectrum simulation has been performed on the geometries optimized in methanol and chloroform solvents, respectively. The electronic properties such as ionization potential, electron affinity, co-efficient of highest occupied molecular orbital (HOMO), co-efficient of lowest unoccupied molecular orbital (LUMO), and band gaps were also calculated at B3LYP/6-31G(d). The band gap was taken as the difference in energies of HOMO and LUMO.

2.2 Characterization of Compound 1

Gummy solid; $\text{C}_{19}\text{H}_{24}\text{O}_2$. $[\alpha]_D^{25} = +25.1$ ($c = 4.6$, CHCl_3). UV (MeOH) λ_{max} : 208 nm (3.1). IR (KBr) ν_{max} 1765 (γ -lactone), 1655 (C=C), 918 cm^{-1} . ^1H -NMR (400 MHz, CDCl_3) (Table-1) and ^{13}C -NMR (100 MHz, CDCl_3) (Table-1). EI-MS m/z : (rel. int.) 284 [M^+] (100), 266 (30), 256 (70), 240 (65), 225 (50), 198 (85), 183 (95), 144 (80), 137 (90), 84 (40). HR-EI-MS: m/z calculated for $\text{C}_{19}\text{H}_{24}\text{O}_2$: 284.1770, found 284.1748.

3. Results and Discussion

3.1. Structure elucidation

The CHCl_3 soluble fraction of the whole plant of *Stachys parviflora* was subjected to column chromatography to give a new rosane-diterpenoid.

Compound **1** (Figure 1a) was isolated as a gummy solid and the molecular formula $\text{C}_{20}\text{H}_{24}\text{O}_2$ was assigned to it based on ^1H - and ^{13}C -NMR spectra and HR-EIMS (M^+ m/z 284.1748). The IR spectrum of compound **1** afforded absorption bands at 1765, 1655, and 918 cm^{-1} suggesting the presence of a γ -lactone and olefin functionalities while its UV spectrum showed absorption maximum at 208 nm indicating the presence of conjugated π -bonds.

The ^1H -NMR spectroscopic data (Table 1) of compound **1** displayed the presence of two methyl singlets at δ_{H} 1.05 (3H, H-17) and 1.07 (3H, H-19), and five olefinic proton signals at δ_{H} 5.25 (1H, m, H-1), 6.42 (1H, m, H-3), 5.40 (1H, dd, $J = 17.4, 10$ Hz, H-15), 5.03 (1H, dd, $J = 16.8, 1.3$ Hz, H-16), and 4.98 (1H, dd, $J = 10.8, 1.3$ Hz, H-16). The spectrum also showed three methine proton signals at

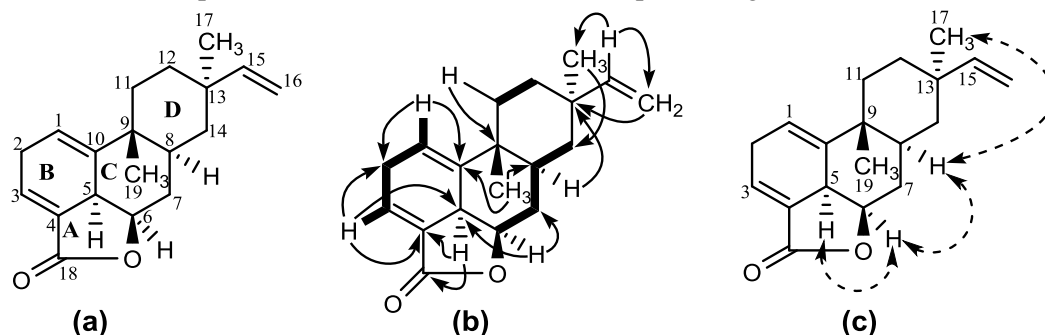


Figure 1. (a). Structure of compound **1** (b). ^1H — ^1H COSY and HMBC (H→C) correlations of compound **1**; (c). NOESY correlations of compound **1**.

δ_{H} 3.01 (1H, d, $J = 7.1$ Hz, H-5), 3.75 (1H, m, H-6), and 1.82 (1H, m, H-8).[13, 14] The ^{13}C -NMR spectrum (BB and DEPT) (Table 1) exhibited 19 carbon signals consisting of two methyl, six methylene, six methine, and five quaternary carbons. The signals in the upfield region at δ_{C} 23.1 and 20.5 were due to methyls while the peak in the downfield region at δ_{C} 173.1 was assigned to the carbonyl carbon. The ^1H - ^1H correlation spectroscopy (COSY) showed correlations between δ_{H} 5.25 (H-1) and δ_{H} 2.20-2.29 (H-2), and between δ_{H} 2.20-2.29 (H-2) and δ_{H} 6.42 (H-3) (Figure 1b) which permitted the position of H-1 and H-3 in the proposed structure.

Table 1. ^1H -NMR data (in CDCl_3) and ^{13}C -NMR of compound **1** in ppm and J in Hz. Chemical shifts in ppm.

Position	^1H -NMR (δ) and multiplicity	(δ) ^1H -NMR calculated at B3LPY/6-311+G(2d,p) (Scaled)	^{13}C -NMR (δ)	(δ) ^{13}C -NMR calculated at B3LPY/6-311+G(2d,p)
1	5.25, m	5.55	119.9	128.4
2	2.20-2.29, m	2.96-3.06	38.4	34.92
	1.25, m			
3	6.42, m	6.88	135.6	147.23
4	-	-	142.1	141.21
5	3.01, d, $J = 7.1$ Hz	3.30	42.4	45.09
6	3.75, m	4.66	85.1	83.53
7	1.76, m	1.36, 1.62	33.2	35.71
8	1.82, m	1.58	38.6	39.49
9	-	-	44.4	45.87
10	-	-	150.7	162.93
11	1.31, m	1.61	36.6	40.71
	1.43, m			
12	1.10, m	1.12, 1.64	35.1	37.08
	1.47, m			
13	-	-	37.9	45.08
14	1.18-1.23, m	1.48-0.93	42.8	42.86
15	5.40 dd, $J = 17.4, 10$ Hz	5.75	153.8	162.05
16	5.03, dd, $J = 16.8, 1.3$ Hz	4.65-4.79	107.7	113.19
	4.98, dd, $J = 10.8, 1.3$ Hz			
17	1.05, s	1.09	23.1	20.41
18	-	-	173.1	176.5
19	1.07, s	0.91	20.5	21.83
-	-	-	-	-

Furthermore, the HMBC spectrum of compound **1** showed ^1H - ^{13}C correlations (Figure 1b) of the methine proton H-1 with C-2 (δ_{C} 38.4) and C-10 (δ_{C} 150.7), while the olefinic proton H-3 showed correlations with C-2, C-4 (δ_{C} 142.1) and C-5 (δ_{C} 42.4) showing the position of double bond between C-3 and C-4. Similarly correlations of H-17 with C-13 (δ_{C} 37.9) and C-14 (δ_{C} 42.8) were also observed. The position of methylene side chain was deduced from the correlation of the olefinic proton H-15 with C-16 (δ_{C} 107.7), and the location of methyl group (C-19) was found to be on C-9 due to the observed correlations of H-19 to C-9 (δ_{C} 44.4), C-10 (δ_{C} 150.7), and C11 (δ_{C} 36.6).

The relative configuration of compound was resolved from its spectral data as well as comparison with the literature. [13-15] Nuclear Overhauser effect spectroscopy (NOESY) experiments established correlations of H-5 (δ_{H} 3.01) to H-6 (δ_{H} 3.75), H-6 to H-8 (δ_{H} 1.82), and H-8 to CH_3 -17 (δ_{H} 1.05) showing these groups to be positioned in the same plane (Figure 1c) consistent with a *cis* relationship between these groups. These results and the fact that the irradiation of CH_3 -19 did not cause any increase in the intensities of the H-5, H-6, H-8, and CH_3 -17 signals confirmed the β -orientation of CH_3 -19.

3.2. Optimized Geometry of Compound **1**

The structure of compound **1** was assigned based on spectroscopic techniques including UV-Vis, IR, ^1H -NMR, ^{13}C -NMR, 2D-NMR techniques. To gain further detailed insight into the structure, DFT

calculations have been performed. The structure of the compound with the correct stereochemistry was optimized at B3LYP method of DFT using 6-31G(d) basis set. The optimized geometry is shown in Figure 2a and important structural parameters are presented in Table 2.

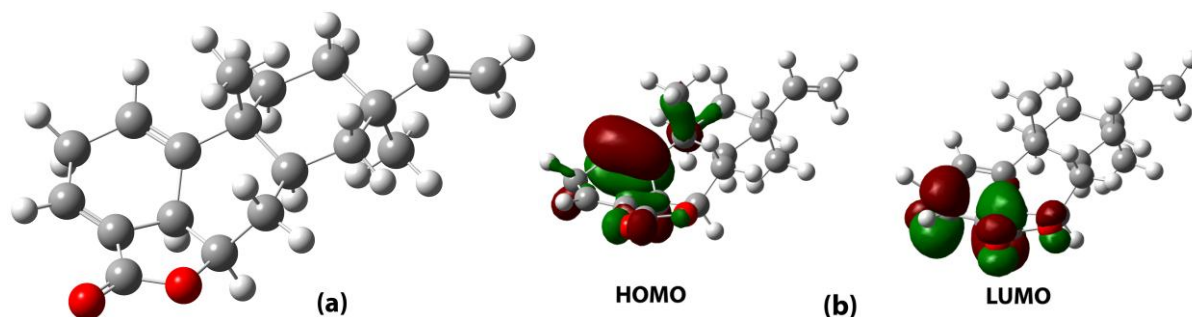


Figure 2(a). Optimized geometry of compound **1** at B3LYP/6-31G*; (b). HOMO and LUMO of compound **1**, calculated at B3LYP/6-31G*. The orbitals are plotted at isodensity of 0.04.

The five membered lactone ring (ring A, see Figure 1a for label) is planar whereas the Ring B is almost boat like. Presence of two double bonds combined with the stereochemistry at carbon 5 render the ring B to adopt boat conformation. Rings C and D are chair like; however, the ring C is a distorted chair.

Table 2. Selected optimized geometric parameters of compound **1**, calculated at B3LYP/6-31G* (refer to Figure 1a for numbering scheme)

Atoms	Bond lengths (Å)	Atoms	Angle (°)
C1-C10	1.34	C1-C2-C10	123.2
C3-C4	1.33	C4-C18-O(carbonyl)	129.47
C18-O	1.21	C4-C18-O	108.01
C18-O	1.37	C2-C1-C10-C9	171.9
C15-C16	1.33	C1-C10-C6-C5	155.65
O-C6	1.45	C3-C4-C5-C10	36.85

3.3. Infra-red Spectral Analysis

The experimental IR spectrum of compound **1** showed prominent peaks for olefinic C-H, aliphatic C-H, lactone C=O, and C=C stretching vibrations in the functional group region. The IR spectrum was also simulated in the gas phase at B3LYP/6-31G(d) and compared with the experimental spectrum. A scaling factor of 0.9613 was applied to the simulated values for better correlation with the experimental results. Four simulated stretching vibrations of C-H bonds on olefinic moieties are 3117, 3078, 3055, and 3047 cm^{-1} . The 3117 and 3047 cm^{-1} vibrations are due to *anti*-symmetric and symmetric stretchings, respectively, of C(16)-H bond. The simulated peak at 1789 cm^{-1} corresponds to C=O stretching vibration and correlates nicely to the experimental 1765 cm^{-1} . The simulated C=C stretching vibrations are 1688, 1657, and 1608 cm^{-1} , mainly due to the presence of three olefinic moieties. The olefinic C=C stretching vibrations are observed experimentally as a broad band at 1655 cm^{-1} .

3.4. UV-Vis Analysis

UV-Vis spectra of compound **1** have been investigated theoretically and experimentally. The experimental spectrum was measured in methanol solvent whereas the simulated spectra were modeled in gas phase, and in chloroform and methanol solvents. The experimental λ_{max} was observed at 208 nm in methanol solvent, however the calculated λ_{max} at TDDFT (B3LYP/6-31G(d)) was 193 nm in the same solvent. The λ_{max} is not much affected by changing the nature of solvent. For example, λ_{max} values are 189 and 196 nm in chloroform and gas phase, respectively. Analysis of the orbitals indicate that the above

transition correspond to π - π^* . The nature of the transition is also consistent with the observed effect of solvent on the absorption spectra.

The highest occupied molecular orbital (HOMO) and lowest unoccupied molecular orbital (LUMO) were also analyzed (Figure 2b). According to Koopman theorem, energies of HOMO and LUMO can be approximately taken equivalent to ionization energy and electron affinity, respectively. The calculated HOMO-LUMO gap was 5.25 eV for compound **1**. The high value of the band gap is indicative of the stability of the molecules towards oxidation and reduction. Both, HOMO and LUMO are mainly centered on the alkene moieties. The HOMO is mainly centered on C1=C10 double bond whereas the LUMO is located on C3=C4 double bond with some density on the lactone moiety.

3.5. NMR Analysis

The ^1H -NMR spectrum of compound **1** was experimentally measured in CDCl_3 on a 400 MHz spectrometer. The theoretical NMR was calculated at B3LYP/6-311+G(2d,p) in chloroform. The chemical shifts were also simulated at B3LYP/6-31G(d) and WP04/6-31G, however, the correlation with the experiment was relatively weak (see supporting information for the details). The NMR was calculated using GIAO formalism, and the solvent effect was introduced through polarizable continuum model (PCM) by applying integral equation formalism. A comparison of the theoretical ^1H - and ^{13}C -NMR values with the experimental values is given in Table 1. A better correlation with the experiment can be achieved if a scaling factor is applied to the ^1H -NMR theoretical values. The scaled values are given in Table 1, whereas unscaled chemical shifts are given in the supporting information. The theoretical ^1H -NMR values are, on the average, higher than the experimental values. Despite the difference in the absolute values, the trend in the chemical shift of the theoretical values matches nicely with the experimental values. The calculated chemical shifts of alkene protons are slightly higher than the experimental values whereas the calculated chemical shifts of aliphatic protons are towards lower end. The chemical shift of the local isomer were also calculated at B3LYP/6-311+G(2d,p) and they are not significantly different than the global minimum (See supporting information)

The calculated ^{13}C -NMR chemical shifts of compound **1** correlate nicely with the experimental chemical shift values, without any scaling factor. The carbonyl carbon (C-18) has the calculated chemical shift of 176.5 which matches nicely with the experimental 173.1. Moreover, the calculated chemical shift for C-6 is 83.5, and it correlates nicely with 85.1. The calculated chemical shifts are within 3 ppm except C-10 and C-15 where this difference rises to about 10 ppm. The difference in calculated and experimental chemical shifts of alkene carbon probably illustrates the inability of the B3LYP methods in accurately describing the alkene motifs.

Conclusion

We have presented a comprehensive theoretical and experimental study of a new rosane type diterpenoid isolated from the ethyl acetate soluble fraction of *Stachys parviflora*. Its structure elucidation was based primarily on 1D- and 2D-NMR techniques. Geometry optimization and vibrational spectral calculation were performed at B3LYP method of DFT using 6-31G* basis set. The calculated vibrational spectrum was scaled with a scaling factor of 0.9613, and the scaled band peak values showed nice correlation with the experimental spectrum. The simulated UV-Vis spectrum in methanol solvent agrees nicely with the experimental spectrum. ^1H - and ^{13}C -NMR spectra were modeled at B3LYP/6-31G(d), B3LYP/6-311+G(2d,p) and Cramer reparameterized WP04/6-31G(d) levels of theories out of which the prominent and more consistent results were obtained at B3LYP/6-311+(2d,p) which were better than the other two theoretical levels under consideration. The calculated ^{13}C -NMR values showed nice correlation with the experimental spectrum without any scaling factor applied; however, the calculated ^1H -NMR values were scaled with a scaling factor of 0.92.

Acknowledgments

We acknowledge the Higher Education Commission (HEC) of Pakistan and COMSATS for financial support.

Supporting Information

Supporting Information accompanies this paper on <http://www.acgpubs.org/RNP>

References

- [1] V. U. Ahmad, S. Arshad, S. Bader, A. Ahmed, S. Iqbal and R. B. Tareen (2006). New phenethyl alcohol glycosides from *Stachys parviflora*, *J. Asian Nat. Prod. Res.* **8**, 105-111.
- [2] P. C. H. Holiman, M. G. L. Hertog and M. B. Katan (1996). Analysis and health effects of flavonoids, *Food Chem.* **57**, 43-46.
- [3] Z. Amirghofran, M. Bahmani, A. Azadmehr and K. Javidnia (2006). Anticancer effects of various Iranian native medicinal plants on human tumor cell lines, *Neoplasma* **53**, 428-433.
- [4] M. J. Frisch, G. W. Trucks, H. B. Schlegel, G. E. Scuseria, M. A. Robb, J. R. Cheeseman, G. Scalmani, V. Barone, B. Mennucci, G. A. Petersson, H. Nakatsuji, M. Caricato, X. Li, H. P. Hratchian, A. F. Izmaylov, J. Bloino, G. Zheng, J. L. Sonnenberg, M. Hada, M. Ehara, K. Toyota, R. Fukuda, J. Hasegawa, M. Ishida, T. Nakajima, Y. Honda, O. Kitao, H. Nakai, T. Vreven, J. Montgomery, J. A., J. E. Peralta, F. Ogliaro, M. Bearpark, J. J. Heyd, E. Brothers, K. N. Kudin, V. N. Staroverov, R. Kobayashi, J. Normand, K. Raghavachari, A. Rendell, J. C. Burant, S. S. Iyengar, J. Tomasi, M. Cossi, N. Rega, J. M. Millam, M. Klene, J. E. Knox, J. B. Cross, V. Bakken, C. Adamo, J. Jaramillo, R. Gomperts, R. E. Stratmann, O. Yazyev, A. J. Austin, R. Cammi, C. Pomelli, J. W. Ochterski, R. L. Martin, K. Morokuma, V. G. Zakrzewski, G. A. Voth, P. Salvador, J. J. Dannenberg, S. Dapprich, A. D. Daniels, Ö. Farkas, J. B. Foresman, J. V. Ortiz, J. Cioslowski and D. J. Fox (2010). Gaussian 09 Revision C. 01, *Gaussian Inc.; Wallingford CT*.
- [5] P. C. Hariharan and J. A. Pople (1973). The influence of polarization functions on molecular orbital hydrogenation energies, *Theoret. Chim. Acta.* **28**, 213-222.
- [6] A. D. Becke (1988). Density-functional exchange-energy approximation with correct asymptotic behavior, *Phys. Rev. A.* **38**, 3098-3100.
- [7] C. Lee, W. Yang and R. G. Parr (1988). Development of the Colle-Salvetti correlation-energy formula into a functional of the electron density, *Phys. Rev. B.* **37**, 785-789.
- [8] G. Barone, L. Gomez-Paloma, D. Duca, A. Silvestri, R. Riccio and G. Bifulco (2002). Structure validation of natural products by quantum-mechanical GIAO calculations of ¹³C NMR chemical shifts, *Chem. Eur. J.* **8**, 3233-3239.
- [9] J. Casado, V. Hernández, F. J. Ramı and J. T. López Navarrete (1999). Ab initio HF and DFT calculations of geometric structures and vibrational spectra of electrically conducting doped oligothiophenes, *J. Mol. Struct. THEOCHEM.* **463**, 211-216.
- [10] M. W. Lodewyk, M. R. Siebert and D. J. Tantillo (2011). Computational prediction of ¹H and ¹³C chemical shifts: A useful tool for natural product, mechanistic, and synthetic organic chemistry, *Chem. Rev.* **112**, 1839-1862.
- [11] R. Jain, T. Bally and P. R. Rablen (2009). Calculating accurate proton chemical shifts of organic molecules with density functional methods and modest basis Sets, *J. Org. Chem.* **74**, 4017-4023.
- [12] P. R. Rablen, S. A. Pearlman and J. Finkbiner (1999). A comparison of density functional methods for the estimation of proton chemical shifts with chemical accuracy, *J. Phys. Chem. A.* **103**, 7357-7363.
- [13] L. K. Mdee, R. Waibel, M. H. H. Nkunya, S. A. Jonker and H. Achenbach (1998). Rosane diterpenes and bis-dinorditerpenes from *Hugonia casteneifolia*, *Phytochemistry* **49**, 1107-1113.
- [14] P. Khiev, S.-R. Oh, H.-S. Chae, O.-K. Kwon, K.-S. Ahn, Y.-W. Chin and H.-K. Lee (2011). Anti-inflammatory diterpene from *Thysanthera suborbicularis*, *Chem. Pharm. Bull.* **59**, 382.
- [15] V. U. Ahmad, U. Farooq, A. Abbaskhan, J. Hussain, M. A. Abbasi, S. A. Nawaz and M. I. Choudhary (2004). Four new diterpenoids from *Ballota limbata*, *Helv. Chim. Acta.* **87**, 682-689.

ACG
publications

© 2015 ACG Publications